Solar Energy based Hybrid Electric Car: Part 2

Dr. Siva Ganesh Malla[1*], Priyanka Malla[2] and Rjesh Koilada[3]

[1]Director, CPGC Pvt. Ltd., Visakhapatnam, Andhra Pradesh, India. Email: mallasivaganesh@gmail.com
[2]Jr. GIS Engineer, Infotech, Cyient Ltd., Vizag, Andhra Pradesh, India, Email: priyamallaece@gmail.com
[3]Det. of Mechanical Engineering, BITS, Vizag, Andhra Pradesh, India, Email: mechkrajesh@gmail.com

Abstract: This paper presents the implementation and controlling strategies of solar energy based Hybrid Electric Car (HEC). The research has presented in three parts due to restriction on length of the article. The analysis of the solar power based HEC is presented in part-1 and results carried out with different possible cases are discussed in part-3. The proposed hybrid electric car which is driven by a 3 phase induction motor powered by using two power sources is designed. In present day scenario the world is looking for solar energy as source based electric cars. But solar (Photovoltaic (PV) cells) itself cannot provide sufficient power to the cars for applications of long drive. So, the alternate power source is mandatory. For consideration of economic issues and long drive applications, incorporate battery is integrated to the system with proper controller. So, the system makes hybrid and more reliable. The MPPT (maximum power point tracing) controller is incorporated to the system by using P&O (perturbation and observation) algorithm which can be utilized for PV system to operate at maximum power level. The model used for vector control deign can be obtained by using the space vector modulation technique. The detailed control logics and models are implemented in MATLAB simulnik platform. The role of bidirectional DC to DC converter and vector control of induction motor has discussed in this part. The relative results are discussed in part 3. The model can be further extended with eletrolyzer and fuel cell systems to operate the car for long drive application.

Keywords: Hybrid Electric Car, Vector Control, Induction Motor, MPPT, Solar Powered Vehicles, Photovoltaic Cells, Modeling of Battery.

Article information:
Article received: June 2019, Revised: Nov 2019, Accepted: Dec 2019. *Corresponding author

Cite this article as: Dr. Siva Ganesh Malla, Priyanka Malla and Rajesh Koilada, "Solar Energy based Hybrid Electric Car: Part 2", *International Journal of New Technologies in Science and Engineering* (IJNTSE), Vol. 6, Issue 6, pp. 26- 38, Dec. 2019.

I. CONTROLLERS ON DC SIDE

The system description, size of components and modeling of different type of components in solar based Hybrid Electric Car (HEC) are presented in part 1. The overview and details of controllers of proposed system will be discussed in this paper. In order to maintain effective control of the inverter, first the dc link voltage which is input to the inverter needs to be regulated. However, the PV output voltage is not being constant, it will vary accordingly load and irradiance [1-2]. According to power and voltage curves of solar PV cells, it can be delivering the maximum power at a particular operating voltage (called as V_{mpp}) [1-4]. The power vs voltage characteristic curve is shown in Fig. 1(a). The PV system can be operated at maximum power point (MPP) level by using power electronics converter with proper maximum power point tracking (MPPT) algorithm. Therefore, maximum power point trackers (MPPTs) are employed to the system for track the peak power from PV systems for best utilization. MPPT is basically a power electronic based converter whose regulate the dc-link voltage of PV corresponding to V_{mpp}, so that the system operates at the MPP [1-9].

The PV power can vary from zero to maximum according to Fig. 1. The maximum generated power by PV system depends on dc-link voltage (i.e, V_{mpp}). Hence, in order to control the dc-link voltage, the physical MPPT converter (i.e, dc-dc converter) is required for regulating the dc-link voltage. In case of battery storage system, a bidirectional DC to DC converter regulates the dc-link voltage and also its acts as MPPT for PV system. In this proposed system, the MPPT algorithm and controller is integrated to bidirectional DC to DC converter, hence it can be act as MPPT of PV system. Hence, bidirectional DC to DC converter not only regulates the DC bus voltage, it also acts as MPPT for PV. Hence, there will not be any extra converter required for PV system to operate as MPPT, it can be reduce the cost, size and weight of the system. Hence, load on battery will reduce and helps to run the car for some more distance. Of the several algorithms of MPPT, P&O algorithm is most popular and extensively used, which is shown in Fig. 1(b) [5]. The following equation is followed to locate the voltage at which the MPP is reached [5].

$$V_{mpp}(k) = V_{mpp}(k-1) + M \times \text{sign}\left(\frac{\text{dp}}{\text{dv}}\right) \tag{1}$$

where, M is steep voltage and k is the iteration and dp/dv is change in PV power with respect to PV voltage.

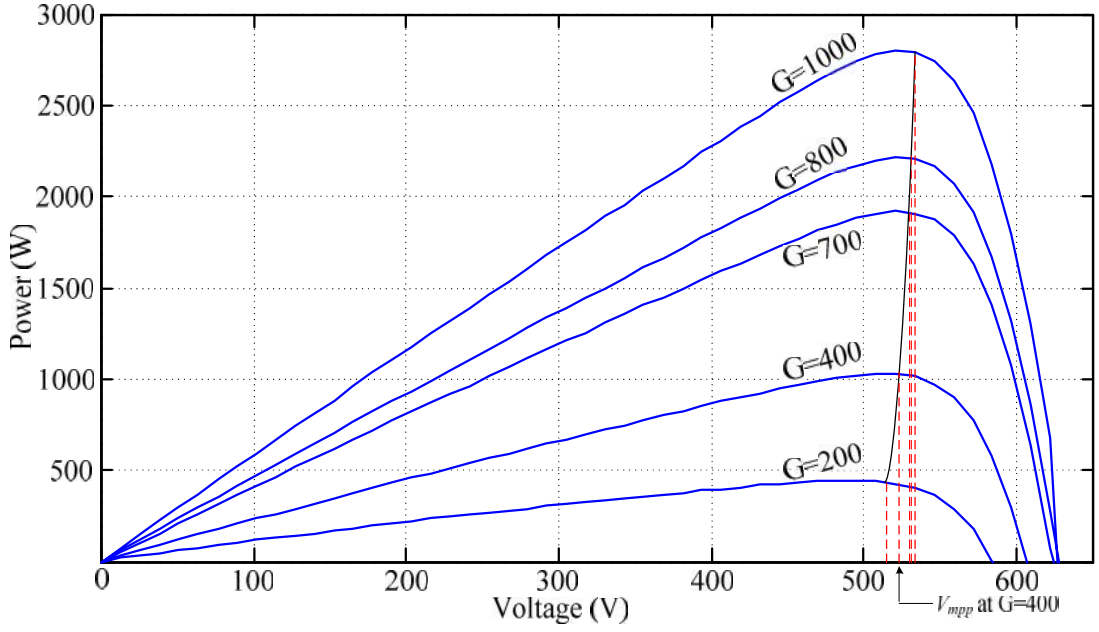

(a)

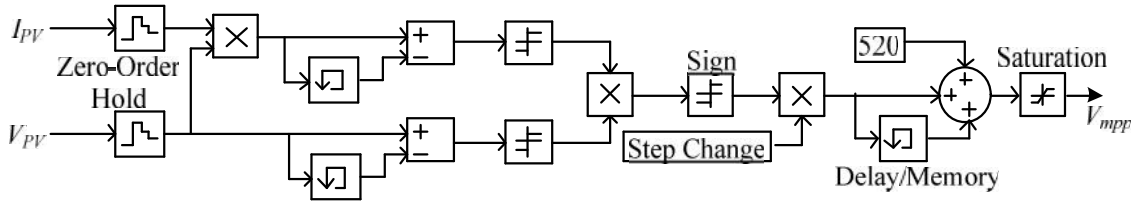

(b)

Fig. 1: (a) P-V curve, (b) P&O algorithm

To achieve the maximum power from PV, a bidirectional dc to dc converter is connected in between PV system and dc link voltage. The PV system output power will be vary according to solar irradiance. Hence, the output voltage of PV system will also vary. The controller is designed to operate the system with MPPT point by regulating the current of battery through bidirectional DC to DC converter by operating the dc link voltage at V_{mpp}. This can be achieved by adjusting the duty cycle of bidirectional DC to DC converter. The proposed controller of bidirectional DC to DC converter of

battery is showing in Fig. 2. Now the responsibility of the control scheme is to produce a reference current which needs to be followed by the battery current. The dc link voltage is compared to V_{mpp} and the error signal is given to Proportional and Integral (PI) controller. The output of the PI controller is generating reference battery current (I^*_{bat}). The reference battery current so obtained is then compared with actual battery current (I_{bat}) and the error is processed through a hysteresis band which in turn gives control signals (gating pulses) to the IGBT devices (S_1 & S_2) of the bidirectional DC to DC converter.

The P&O algorithm will generate the reference voltage (V_{mpp}) as shown in Fig. 1.Depending upon the sign of change in power with respect to sign of voltage, the direction for further perturbation is decided. This reference voltage signal will be sent to DC to DC controller as a reference voltage signal. The following equation is followed to locate the voltage at which the MPP is reached.

$$V_{mpp}(k) = V_{mpp}(k-1) + \Delta V \times \text{sign}\left(\frac{dP_{PV}}{dV_{PV}}\right) \quad (2)$$

Where, ΔV is steep voltage and k is the iteration.

The bidirectional DC to DC converter interfaces the low-voltage battery with a high-voltage dc bus and maintains a bidirectional power flow [1, 10]. In order to increase the life time of the battery, a state of charge (SOC) based controller is implemented as shown in Fig. 2. The dc-link voltage is controlled within a limit so that the actual charging/discharging current will be as per the given specifications. There are three operating modes in bidirectional DC to DC converter i.e. plug-in AC/DC charging of battery, Boost operation from the low-voltage of battery to the high-voltage bus of the EV, and buck operation from the high-voltage bus to the battery for regenerative charging. The dc link is connected with battery through a bidirectional DC to DC converter. By using bidirectional converter, the battery voltage can be able to kept at lower as compared to reference dc link voltage (V^*_{dc}) and hence we can reduce the number of batteries connected in series. In this proposed system the battery voltage is about 300 V while V^*_{dc} = 526V, it is the rating of the high energy battery, as considering 90% depth of discharge (DOD). By considering the output of a controller as the reference current for the battery, a hysteresis band approach is adapted to switch either S_1 or S_2 of the bidirectional converter. Moreover, the control signal is inhibited within a limit so that the actual charging /discharging current will be as per the specification of the battery. Therefore, the dc bus voltage should maintain high enough to match the motor voltage rating.

If SOC of the battery reaches 95%, then the battery will be disconnected from charging operation and PV can adjust the voltage at its power level. The voltage signal at maximum power point of the PV is coming from P and O algorithm and it is giving as an input to bidirectional dc to dc converter. Hence, the bidirectional dc to dc converter reference signal will be the V_{mpp} of the PV system. This reference voltage signal is comparing with actual dc link voltage (i.e., output of the PV or input of the inverter) signal. The error is given to PI controller. The PI controller will generate the reference battery current depends on voltage level on DC side. Actually power mismatch will be reflected in change in voltage on dc link. This reference battery current is now comparing with actual battery current and pulses will be generated with the help of hysteresis band. The pulses will operate the switches and can control the duty cycle of the bidirectional DC to DC converter. Moreover, the SOC also incorporated to controller to improve the life cycle of the battery. The details controller circuit is shown in Fig. 2.

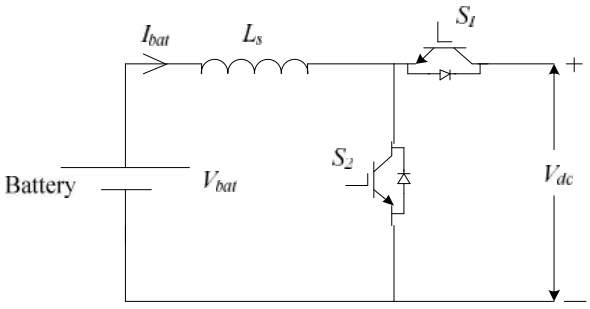

(a): Bidirectional DC to DC Converter

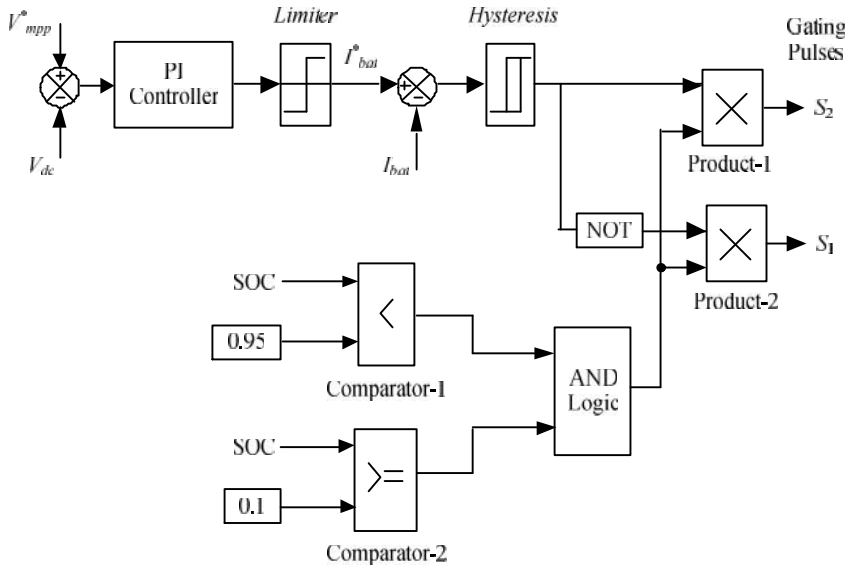

(b): DC-DC Converter control

Fig. 2: (a) Bidirectional DC to DC Converter, (b) DC to DC converter control

II. CONTROLLER ON AC SIDE

The Induction motor is connected through inverter. To run the vehicle, the wheels needs to driven by induction motor only. The motor plays a very important role in hybrid electric vehicle. The smooth operation of vehicle will be depends on control of the induction motor only. Hence, the speed torque characteristics should be identical and should not be depends on each other to run the vehicle at different speeds with same torque and vice versa. This type of capabilities are available in separately excited DC motor, however, already we mentioned the reasons to select the induction motor in previous part, i.e. part 1. Hence, considered that by using vector control, the induction motor can runs as a separately excited motor. In this section, the details concept and implementation of vector control is presented.

Ideally, a vector controlled induction motor drive operates like a separately excited dc motor drives. The armature current and field current are orthogonal or decoupled in nature. This means that when torque is controlling the armature current and field current is controlled when speed control is needed. The comparisons are shown in Fig. 3 [11-12].

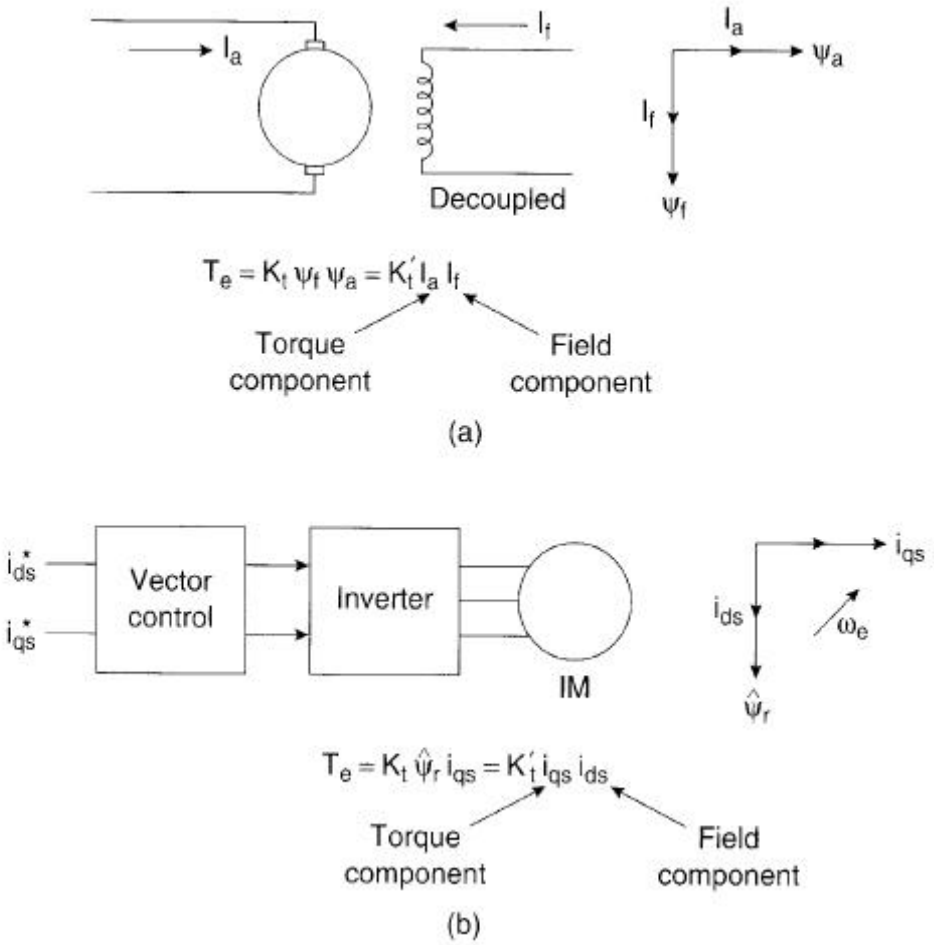

Fig. 3: (a): separately excited DC motor, (b) Vector controlled Induction motor.

DC machine performance is suitable for electric vehicle applications and it can also be achieved from induction motor if the machine control is considered in as synchronously rotating reference frame. The induction motor with the inverter and vector control in the front end is shown with two control currents, i_{ds}^* and i_{qs}^*. These currents are the direct axis component and quadrature axis component of the stator currents respectively. With vector control, i_{ds} is analogous to field current I_f and i_{qs} is analogous to armature current I_a of a dc machine as shown in Fig. 4.

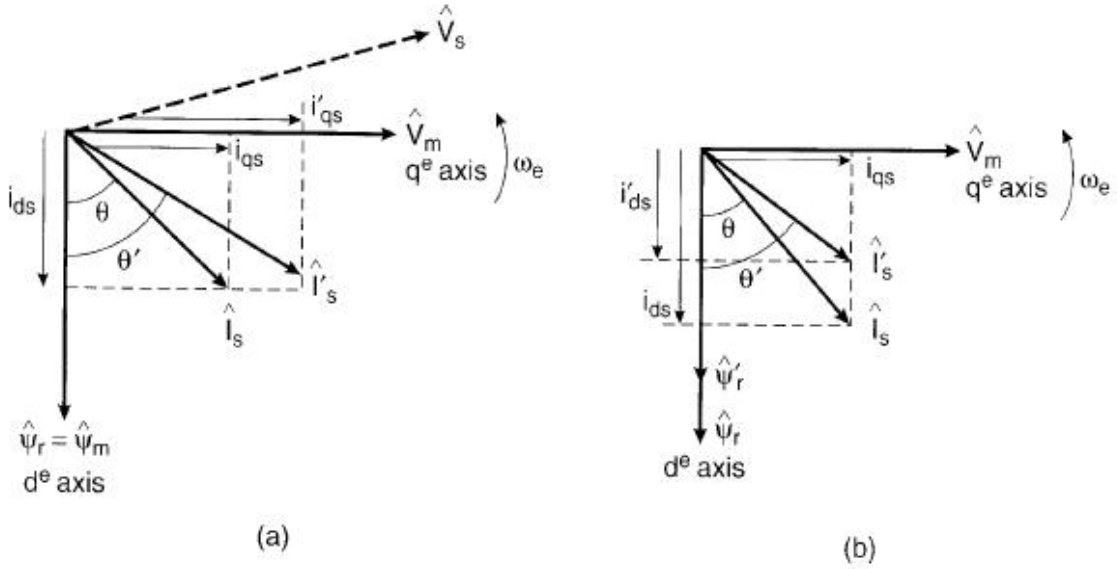

Fig. 4.: Steady state phasors (a) increase of torque component current, (b) Increase of flux component of current.

The principal implementation of vector control is shown in Fig. 5. The inverter is considered as unity current gain, it generates currents i_a, i_b, and i_c as dictated by corresponding command current i_a*, i_b* and i_c* from the controller. A machine model with internal conversations is shown on the right side of the figure. The achieved terminal phase currents i_a, i_b, and i_c are converted to i_{ds} s and i_{qs}. These are then converted to synchronously rotating frame by the unit vector components CosΘe and sineΘe before applying them to the de and qe machine model as shown in Fig. 5. General model of vector control is shown in Fig. 6.

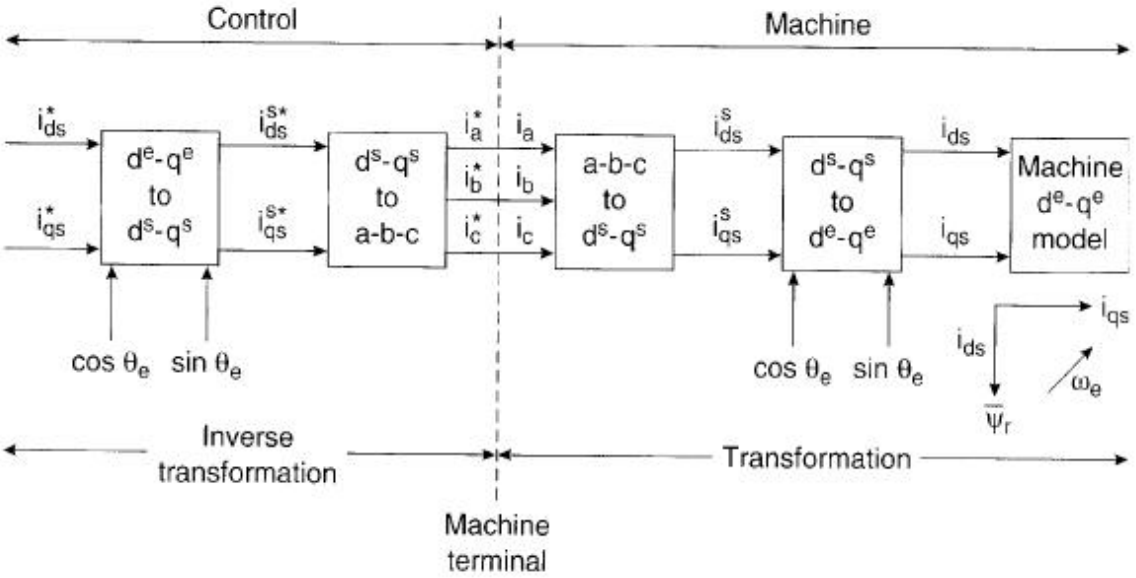

Fig. 5: Vector control implementation principle with machine de and qe model.

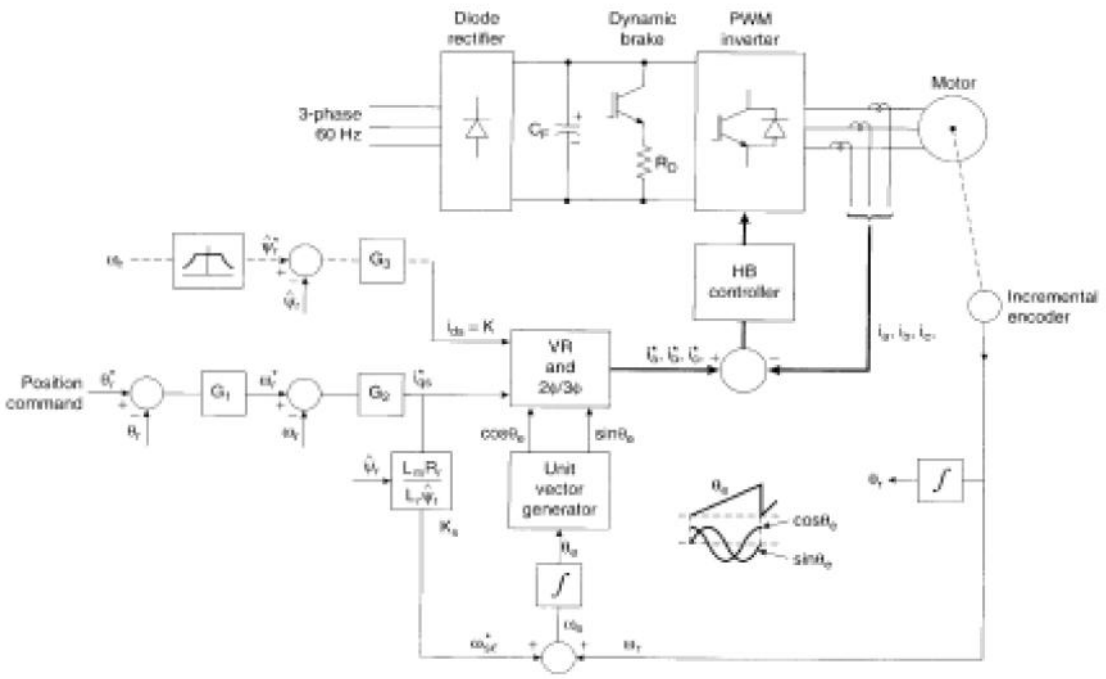

Fig. 6: Detailed vector control model [11]

In [13-15], the authors proposed water pumping system based on scalar control of IM drive. However, scalar control (*v/f*) have limitation that voltage cannot increase beyond the rated value. Due to this limitation frequency cannot increase beyond the rated value for constant torque applications. Scalar control, such as the constant *v/f* method when applied to an IM is relatively simple to implement but it gives a sluggish response because of the inherent coupling effect due to torque and flux being functions of current and frequency. Moreover accurate position control is not possible with scalar control since this requires instantaneous control of the torque. On the other hand, vector control de-couples the vectors of field current and armature flux so that they may be controlled independently to provide fast transient response [11-12]. The three phase motor currents are decomposed into the field component (I_d) and the torque component (I_q). Under such circumstances, the generated torque can be expressed as [11-12]

$$T_e = KI_d I_q \quad (3)$$

Here, I_d is oriented in the direction of flux (Ψ) and I_q is established perpendicular to it. This means that when reference current of I_q (I^*_q) is controlled, it affects the actual I_q current only, but does not affect the flux. Similarly, when reference current of I_d (I^*_d) is controlled, it controls the flux only and does not affect the I^*_q component of current [11-12]. In this thesis, since we are controlling I_q by keeping I_d as constant, the flux will remain constant for various operating conditions.

The dc-link voltage is regulated with switch S_1 and S_2 of bidirectional DC to DC converter and pulse width modulation (PWM) inverter is controlled using vector control (Fig. 7). Therefore, if PV power is more than load, battery can charge and in case of load is more than PV power, battery can discharge to meet the load demand. Once dc link has stabilizing, the inverter controller can easily regulate the speed of induction motor at its reference value. The blocks involved in vector control is shown in Fig. 7.

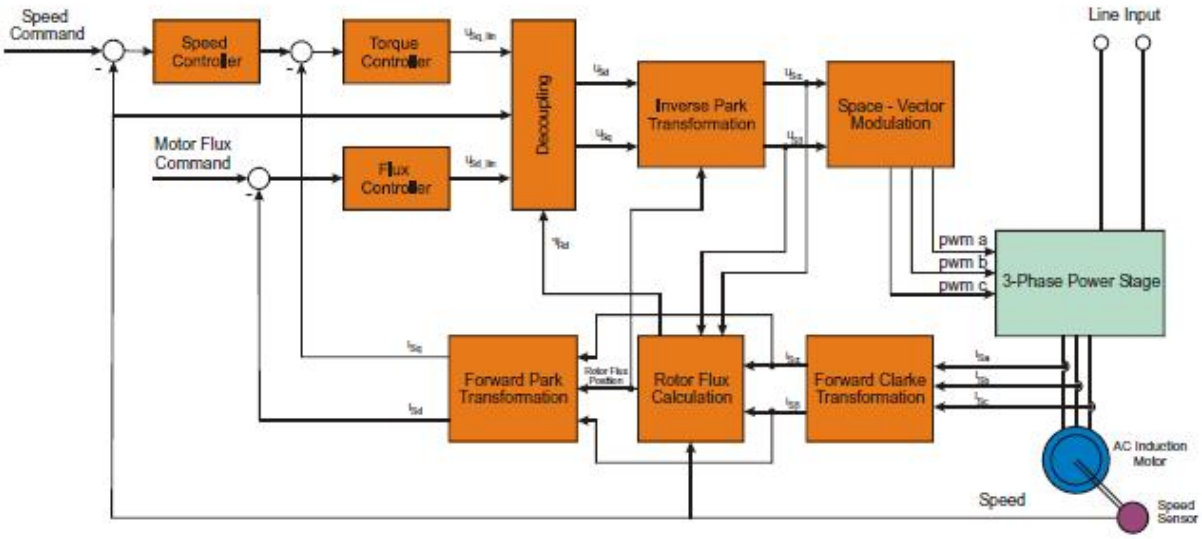

Fig. 7: Forward and Inverse Clarke Transformation (a,b,c to α,β and backwards)

The forward Clarke transformation converts a 3-phase system (a, b, c) to a 2-phase coordinate system (α, β). Fig. 8 shows graphical construction of the space vector and projection of the space vector to the quadrature-phase components α, β.

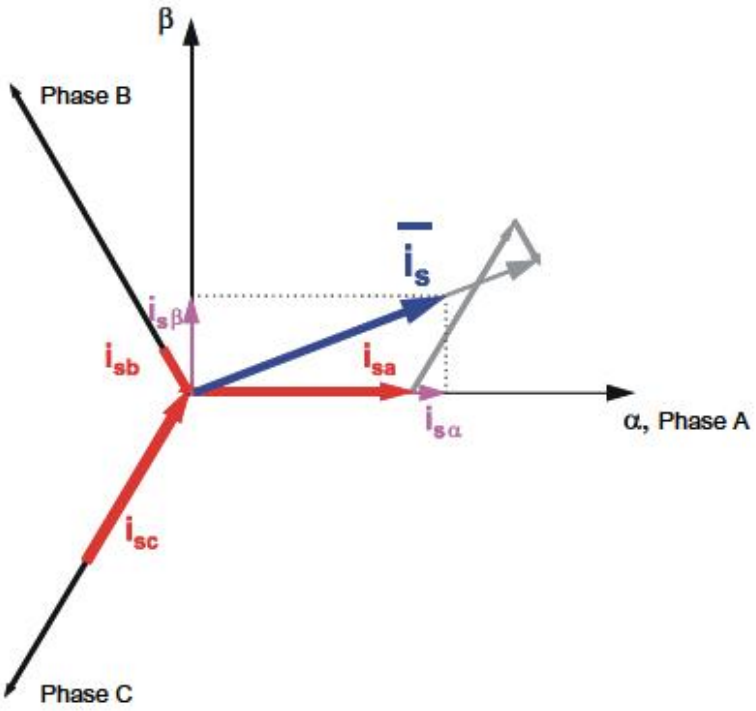

Fig. 8: Clarke Transformation

Assuming that the *a* axis and the α axis are in the same direction, the quadrature-phase stator currents $i_{s\alpha}$ and $i_{s\beta}$ are related to the actual 3-phase stator currents as follows:

$$i_{s\sim} = k\left[i_{sa} - \frac{1}{2} i_{sb} - \frac{1}{2} i_{sc} \right] \tag{4}$$

$$i_s = k \frac{\sqrt{3}}{2} \left[i_{sb} - i_{sc} \right] \tag{5}$$

where:
i_{sa} = Actual current of the motor Phase A [A]
i_{sb} = Actual current of the motor Phase B [A]
$i_{s\alpha,\beta}$ = Actual current of the motor Phase C [A]

The constant k equals $k = 2/3$ for the non-power-invariant transformation. In this case, the quantities i_{sa} and $i_{s\alpha}$ are equal. If it's assumed that, the quadrature-phase components can be expressed utilizing only two phases of the 3-phase system:

$$i_{s\sim} = i_{sa} \tag{6}$$

$$i_s = \frac{1}{\sqrt{3}} i_{sa} + \frac{2}{\sqrt{3}} i_{sb} \tag{7}$$

The inverse Clarke transformation goes from a 2-phase (α, β) to a 3-phase i_{sa}, i_{sb}, i_{sc} system. For constant $k = 2/3$, it is calculated by the following equations:

$$i_{sa} = i_{s\sim} \tag{8}$$

$$i_{sb} = -\frac{1}{2} i_{s\sim} + \frac{\sqrt{3}}{2} i_s \tag{9}$$

$$i_{sc} = -\frac{1}{2} i_{s\sim} - \frac{\sqrt{3}}{2} i_s \tag{10}$$

The components $i_{s\alpha}$ and $i_{s\beta}$, calculated with a Clarke transformation, are attached to the stator reference frame α, β. In vector control, all quantities must be expressed in the same reference frame. The stator reference frame is not suitable for the control process. The space vector is rotating at a rate equal to the angular frequency of the phase currents. The components $i_{s\alpha}$ and $i_{s\beta}$ depend on time and speed. These components can be transformed from the stator reference frame to the d-q reference frame rotating at the same speed as the angular frequency of the phase currents. The i_{sd} and i_{sq} components do not then depend on time and speed. If the d-axis is aligned with the rotor flux, the transformation is illustrated in Fig. 9, where $\theta field$ is the rotor flux position.

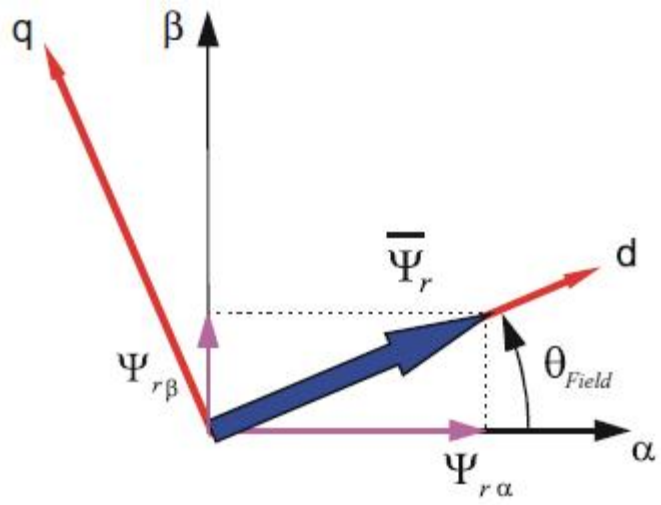

Fig. 9: Park Transformation

The components i_{sd} and i_{sq} of the current space vector in the d-q reference frame are determined by the following equations:

$$i_{sd} = i_{s\sim} \cos^{-}_{Field} + i_{s} \sin^{-}_{Field} \quad (11)$$

$$i_{sq} = -i_{s\sim} \sin^{-}_{Field} + i_{s} \cos^{-}_{Field} \quad (12)$$

The component i_{sd} is called the direct axis component (the flux-producing component) and i_{sq} is called the quadrature axis component (the torque-producing component). They are time invariant; flux and torque control with them is easy. To avoid using trigonometric functions on the hybrid controller, directly calculate $\sin\theta_{Field}$ and $\cos\theta_{Field}$ using division, defined by the following equations:

$$\cdot_{rd} = \sqrt{\cdot^{2}_{r\sim} + \cdot^{2}_{r}} \quad (13)$$

$$\sin^{-}_{Field} = \frac{\cdot_{r}}{\cdot_{rd}} \text{ and } \cos^{-}_{Field} = \frac{\cdot_{r\sim}}{\cdot_{rd}}$$

The inverse Park transformation from the d-q to the α, β coordinate system is found by the following equations:

$$i_{s\sim} = i_{sd} \cos^{-}_{Field} - i_{sq} \sin^{-}_{Field} \quad (14)$$

$$i_{s} = i_{sd} \sin^{-}_{Field} + i_{sq} \cos^{-}_{Field} \quad (15)$$

Knowledge of the rotor flux space vector magnitude and position is key information for AC induction motor vector control. With the rotor magnetic flux space vector, the rotational coordinate system (d-q) can be established. There are several methods for obtaining the rotor magnetic flux space vector. The flux model implemented here utilizes monitored rotor speed and stator voltages and currents. It is calculated in the stationary reference frame (α, β) attached to the stator. The error in the calculated value of the rotor flux, influenced by the changes in temperature, is negligible for this rotor flux model. The rotor flux space vector is obtained by solving the differential equations (16) and (17), which are resolved into the α and β components. The equations are derived from the equations of the AC induction motor model;

$$[(1-\pm)T_s + T_r]\frac{d}{dt}\cdot_{r\sim} = \frac{L_m}{R_s}u_{s\sim} - \cdot_{r\sim} - \mu T_r \cdot_{r} - \pm L_m T_s \frac{d}{dt} i_{s\sim} \quad (16)$$

$$[(1-\pm)T_s + T_r]\frac{d}{dt}\cdot_{r} = \frac{L_m}{R_s}u_{s} - \cdot_{r} + \mu T_r \cdot_{r\sim} - \pm L_m T_s \frac{d}{dt} i_{s} \quad (17)$$

Where:

L_s = Self-inductance of the stator [H]
L_r = Self-inductance of the rotor [H]
L_m = Magnetizing inductance [H]
R_r = Resistance of a rotor phase winding [Ohm]
R_s = Resistance of a stator phase winding [Ohm]
ω = Angular rotor speed [rad.s-1]
P_p = Number of motor pole pairs

$T_r = \frac{L_r}{R_r}$ = Rotor time constant [s]

$T_s = \frac{L_s}{R_s}$ = Stator time constant [s]

$\pm = 1 - \frac{L_m^2}{L_s L_r}$ = Resultant leakage constant [-]

For purposes of the rotor flux-oriented vector control, the direct-axis stator current i_{sd} (the rotor flux-producing component) and the quadrature-axis stator current i_{sq} (the torque-producing

component) must be controlled independently. However, the equations of the stator voltage components are coupled. The direct axis component u_{sd} also depends on i_{sq} and the quadrature axis component u_{sq} also depends on i_{sd}. The stator voltage components u_{sd} and u_{sq} cannot be considered as decoupled control variables for the rotor flux and electromagnetic torque. The stator currents i_{sd} and i_{sq} can only be independently controlled (decoupled control) if the stator voltage equations are decoupled and the stator current components i_{sd} and i_{sq} are indirectly controlled by controlling the terminal voltages of the induction motor.

The equations of the stator voltage components in the d-q coordinate system (16) and (17) can be reformulated and separated into two components:

- Linear components
- Decoupling components

The equations are decoupled as follows:

$$u_{sd} = u_{sd}^{lin} + u_{sd}^{decouple} = \left(K_R i_{sd} + K_L \frac{d}{dt} i_{sd} \right) - \left(\mu_s K_L i_{sq} + \frac{L_m}{L_r T_r} \cdot \Phi_{rd} \right) \tag{18}$$

$$u_{sd} = u_{sq}^{lin} + u_{sq}^{decouple} = \left(K_R i_{sq} + K_L \frac{d}{dt} i_{sq} \right) + \left(\mu_s K_L i_{sd} + \frac{L_m}{L_r} \mu \cdot \Phi_{rd} \right) \tag{19}$$

Where: $K_R = R_s + \frac{L_m^2}{L_r^2} R_r$, $K_L = L_s - \frac{L_m^2}{L_r}$

The voltage components are the outputs of the current controllers which control i_{sd} and i_{sq} components. They are added to the decoupling voltage components to yield direct and quadrature components of the terminal output voltage. This means the voltage on the outputs of the current controllers is:

$$u_{sd}^{lin} = K_R i_{sd} + K_L \frac{d}{dt} i_{sd} \tag{20}$$

$$u_{sq}^{lin} = K_R i_{sq} + K_L \frac{d}{dt} i_{sq} \tag{21}$$

The decoupling components are:

$$u_{sd}^{decouple} = -\left(\mu_s K_L i_{sq} + \frac{L_m}{L_r T_r} \cdot \Phi_{rd} \right) \tag{22}$$

$$u_{sq}^{decouple} = \left(\mu_s K_L i_{sd} + \frac{L_m}{L_r} \mu \cdot \Phi_{rd} \right) \tag{23}$$

As shown, the decoupling algorithm transforms the nonlinear motor model to linear equations which can be controlled by general PI or PID controllers instead of complicated controllers. Space Vector Modulation (SVM) can directly transform the stator voltage vectors from an α, β-coordinate system to Pulse Width Modulation (PWM) signals (duty cycle values).

The detailed vector control modeling is shown in Fig. 10, this can be achieved by above mathematical equations. The speed will be regulated according to reference speed of car, i.e., according to our required speed within limits.

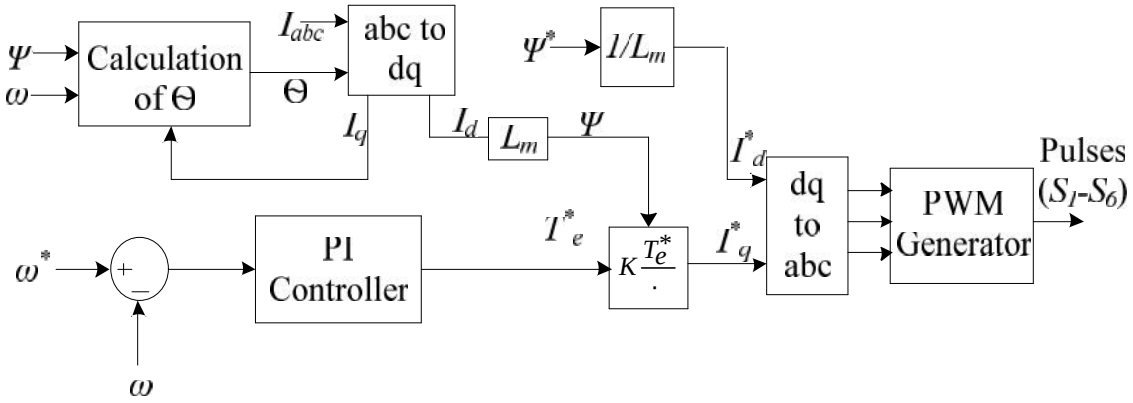

Fig. 10: Block diagram of vector control

The Matlab model of Vector control is implemented by using Fig. 10. The corresponding results with detailed discussion are presented in part 3.

III. CONCLUSION

The analysis of solar powered based HEV has presented in part 1 and the continuous research on controllers of the proposed system is described in this paper as part 2. The regulation of dc link voltage is achieved by controlling of DC to DC converter. Moreover, with the help of integration of P and O algorithm and controller of DC to DC converter, the maximum power from PV system also obtained without any extra converter to get maximum power from PV system like MPPT converter. This can reduce the cost, size and weight of the system hence car can run more distance with same battery capacity. The SCO also incorporated while designing the controller of DC to DC converter to improve the life cycle of battery. With the help of vector control of induction motor, separately excited dc motor characteristics can be obtained which is more suitable for electric vehicles. The detailed modeling of DC to DC converter controller and vector controller has described with the help of mathematical analysis. The signification of controllers also presented in this paper. The results with valid possible cases will be presented in part 3 with the help of controllers presented in this paper.

REFERENCES

[1] S. G. Malla, et al., “Wind and Photovoltaic based Hybrid Stand-Alone Power Generation System”, IEEE: International Conference on Energy, Communication, Data Analytics and Soft Computing (ICECDS 2017),Chennai, India, 2017.

[2] S. G. Malla, et al., “Solar-Hydrogen Energy based Hybrid Electric Vehicle”, IEEE: International Conference on Energy, Communication, Data Analytics and Soft Computing (ICECDS 2017), Chennai, India, 2017.

[3] Aneesha. K and Dr. Priya G Das, “A Non Isolated High step up DC to DC Converter with Continuous Input Current for PV System”, International Journal of New Technologies in Science and Engineering (IJNTSE) , Vol. 5, Issue. 3, pp. 1- 11, May, 2018.

[4] S G Malla, C N Bhende, "Enhanced operation of stand-alone “Photovoltaic-Diesel Generator-Battery” system", Electric Power Systems Research, Vol. 107, pp. 250-257, Feb. 2014.

[5] T. Esram and P. L. Chapman, “Comparison of Photovoltaic Array Maximum Power Point Tracking Techniques”, IEEE Transactions on Energy Conversion, Vol. 22, No. 2, pp. 439-449, June 2007.

[6] D. Sera, R. Teodorescu, J. Hantschel and M. Knoll, “Optimized Maximum Power Point Tracker for Fast-Changing Environmental Conditions”, IEEE Transactions on Industrial Electronics, Vol. 55, No. 7, pp. 2629-2631, July 2008.

[7] C. S. Chiu, "T-S Fuzzy Maximum Power Point Tracking Control of Solar Power Generation Systems", IEEE Transactions on Energy Conversion, Vol. 25, No. 4, pp. 1123-1132, Dec. 2010.
[8] C. S. Chiu and Y. L. Ouyang, "Robust Maximum Power Tracking Control of Uncertain Photovoltaic Systems: A Unified T-S Fuzzy Model-Based Approach", IEEE Transactions on Control Systems Technology, Vol. 19, No. 6, pp. 1516-1526, Nov. 2011.
[9] K. H. Hussein, I. Muta, T. Hoshino and M. Osakada, "Maximum Photovoltaic Power Tracking: an Algorithm for Rapidly Changing Atmospheric Conditions", *IEE* Proc-Generation, Transmission and Distribution, Vol. 142, No. 1, pp. 59-64, Jan.1995.
[10] Nisha. C.K and Priya. S, "Bidirectional DC-DC Converter for Energy Storage Systems", International Journal of New Technologies in Science and Engineering (IJNTSE), Vol. 5, Issue. 3, pp. 12- 21, May, 2018.
[11] Bose B.K, Power Electronics and Motor Drives, Academic Press, Imprint of Elsevier, 2006.
[12] C N Bhende, S G Malla, "Novel control of photovoltaic based water pumping system without energy storage", International Journal of Emerging Electric Power Systems, Vol. 13, Issue 5, Nov. 2012.
[13] J. R. Arribas and C. M. V. González, "Optimal Vector Control of Pumping and Ventilation Induction Motor Drives", IEEE Transactions on Industrial Electronics, Vol. 49, pp. 889–895, Aug. 2002.
[14] M. A. Elgendy, B. Zahawi and D. J. Atkinson, "Assessment of Perturb and Observe MPPT Algorithm Implementation Techniques for PV Pumping Applications", IEEE Transactions on Sustainable Energy, Vol. 3, No. 1, pp. 21-33, Jan. 2012.
[15] A. Betka and A. Moussi, "Performance Optimization of a Photovoltaic Induction Motor Pumping System", Renewable Energy, No. 29, pp. 2167- 2181, 2004.

Dr. Siva Ganesh Malla was born on 1986 in Nagulapalli, Anakapalli, Visakhapatnam, Andhra Pradesh, India. He received the award of Ph. D from School of Electrical Sciences, Indian Institute of Technology (IIT) Bhubaneswar, Odissa, India in 2014. He got his B. Tech degree in Electrical Deportment from Jawaharlal Nehru Technological University Hyderabad in 2007 and M. Tech in Power Electronics and Electric Drives in Electrical Deportment from Jawaharlal Nehru Technological University Kakinada in 2010. Now he is working as a director of CPGC Pvt. Ltd, Visakhapatnam, Andhra Pradesh, India. His research interests are renewable energy sources, microgrid, power quality, electrical vehicles, biomedical signal processing, converters, power electronics, drives, optimization techniques and FACTS.

Priyanka Malla was born on 1996 in Anakapalli, Visakhapatnam, Andhra Pradesh, India. She received her B. Tech in Electronics and Communication Engineering from Jawaharlal Nehru Technological University, Kakinada, India, in 2017. Presently she is working as Jr. GIS Engineer, Infotech, Cyient Ltd., Vizag, Andhra Pradesh, India. Her research interests are included in renewable energy sources, electrical vehicles, biomedical signal processing, optical communication and digital electronics.

Rajesh Koilada was born on 2000 in Venkupallem, Anakapalli, Visakhapatnam, Andhra Pradesh, India. Presently he is working towards his batchlar degree in Mechanical Engineering Department, Baba Institute of Technology and Sciences, affiliated to Jawaharlal Nehru Technological University, Kakinada, India. His research interests are included in renewable energy sources, electrical vehicles, robotics, thermal engineering, fluid dynamics and machine designing.